



Source Impact of a DC/AC Converter on Impedance-based Stability Analysis for Power Hardware-in-the-Loop Setups

Sarah Okumu 

*Institute of Technical Physics (ITEP)
Karlsruhe Institute of Technology (KIT)
Karlsruhe, Germany*

Fargah Ashrafidehkordi 

*Institute of Technical Physics (ITEP)
Karlsruhe Institute of Technology (KIT)
Karlsruhe, Germany*

Giovanni De Carne 

*Institute of Technical Physics (ITEP)
Karlsruhe Institute of Technology (KIT)
Karlsruhe, Germany*

Abstract—Power Hardware-in-the-Loop (P-HIL) provides a controlled environment in a lab to test hardware under realistic operating conditions. Interfaces are implemented to connect the Hardware-of-Interest (HoI) and the digital real-time simulator (DRTS). Delays and noise are introduced through the DRTS and interfaces, which can cause inaccuracy and instability. Before conducting experiments, the stability of P-HIL with a chosen Hardware of Interest must be analyzed to prevent damage to the setup. This paper assesses the stability of a P-HIL setup using an impedance-based modeling approach when the HoI is a grid-following converter. It focuses on the DC port's impact on the stability analysis, whereby the DC port is considered dynamic. To apply the impedance-based stability analysis, the grid and inverter impedances of this setup are modeled and calculated. Through frequency response, the calculated impedances are verified in simulations. The stability criteria for the P-HIL setup are verified by comparing the Nyquist criterion with the time domain response in Simulink/MATLAB.

Index Terms—Power Hardware-in-the-Loop, impedance-based stability, grid-following converter, DC port impact

I. INTRODUCTION

As the amount of renewable energy in the grid increases, the importance of power electronic-based technologies in the grid, such as grid-following, grid-forming converters, and smart transformers, also increases [1] [2]. Having a test environment that provides accurate and reliable test results for a safe integration of new technologies into the grid is essential. A Power Hardware-in-the-Loop (P-HIL) setup can be used to test hardware under realistic operating conditions in a laboratory environment [3] [4]. Recent applications of the P-HIL are testing asynchronous grids [5], virtual motors [6], and the virtual synchronous machine validation in flywheels [7]. Also, new power electronic-based technologies such as smart transformers and grid-tied converters have been tested in P-HIL setups [8] [9]. These examples show the wide variety of possible applications for P-HIL setups.

A P-HIL setup, shown in Fig. 1, includes a digital real-time simulator (DRTS), Hardware-of-Interest (HoI), and interfaces to connect these two components. Digital analog converters,

a power amplifier, and a sensor are part of the interfaces. The DRTS emulates a grid, and the amplifier amplifies the signal from the DRTS and sends it to the HoI. To close the loop, the values at the HoI are measured through sensors and sent back to the DRTS. Because the grid is emulated, it does not have to exist in reality. This enables tests of different grids with the HoI, as only the model in the DRTS has to be changed, but the rest of the setup can remain the same. Using a DRTS to emulate a grid avoids field tests in the real grid, which are hard to realize with new hardware. While a P-HIL setup has many advantages, it also comes with some challenges, as the DRTS and interfaces introduce delays that do not exist when the hardware is directly connected to the real grid. These delays can cause instability and inaccuracy in the setup [10]. To improve the stability and accuracy of a P-HIL setup, different Interface Algorithms (IA) can be implemented [11]. IAs differ in their stability and accuracy, among which the Ideal Transformer Method (ITM) is known for its simplicity in implementation [11]. ITM can be parted in voltage- or current-type depending on whether the reference signal for the amplifier is a voltage or current [12]. Another method to improve the stability of the P-HIL setup can be using a numerical low-pass filter that reduces high-frequency noises in a tradeoff with decreased accuracy [13]. To improve the accuracy of a P-HIL, a multi-rate discrete-time modeling approach can be implemented [14]. As the Hardware of Interest is not very well known and delays can cause instability, the stability of the whole setup needs to be evaluated before conducting experiments to avoid hardware damage. This stability assessment can be done using the impedance-based stability analysis, where a system is partitioned into a source and load subsystem using the Thevenin or Norton equivalent [15]. The impedance-based stability analysis uses the ratio of the source and load impedances measured at PCC to assess the stability of a setup [16]. One advantage of this approach is that it can be used when the hardware is a black box, as it does not need a precise hardware model.

In [17], the impedance-based stability analysis of a P-HIL setup is evaluated when the HoI is a grid-following converter. The analysis was performed assuming that the converter is

This work is supported by the Helmholtz Association under the program "Energy System Design" and the Helmholtz Young Investigator Group "Hybrid Networks" (VH-NG-1613).

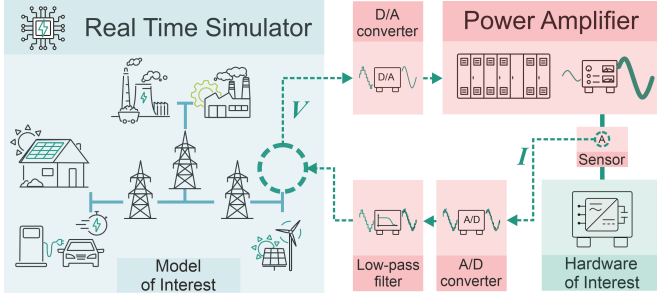


Fig. 1. Structure of P-HIL

connected to an ideal DC link, which means that the DC capacitor has an infinite capacitance. The influence of the DC link dynamics on the setup's stability and, thus also, on the impedance-based stability analysis is neglected.

This paper focuses on the stability of a grid-tied converter in a P-HIL setup with an external DC port and shows the impact of the DC link components on the setup's stability. The impedance-based stability criteria for this setup are examined to provide a reliable method to assess the stability of such P-HIL setups.

The paper is structured as follows: In section II, the components of the complete P-HIL setup used in this paper and the corresponding impedance-based model are introduced. The setup consists of a stiff grid emulated in the DRTS connected to a grid-following converter with an external DC port. From this setup, the grid and inverter impedances are modeled. The modeled impedances are verified through simulation in section III. Lastly, in section IV, the stability criteria for this setup are introduced, and the stability is assessed with the Impedance-based analysis using the Nyquist criterion. The stability analysis is shown when different parameters, like the DC capacitor size, change. The results of this section are verified by comparing them to the benchmark of this setup in Simulink/MATLAB.

II. MODELING

This section shows the impedance-based modeling of a P-HIL setup as the HoI is a grid-following converter considering the DC port dynamics. As an Interface Algorithm, the voltage-type ideal transformer method (V-ITM) is used. The Thevenin equivalent is used for the grid emulated in the DRTS, which comprises a voltage source V_S and an impedance Z_S in series. The current i at PCC can be expressed with the help of the transfer functions of the forward and feedback path of the Interface. The transfer functions of the DRTS, D/A converter and amplifier are considered in the forward path G_{ifw} , where T_{DRTS} , $T_{D/A}$ and T_{amp} are the respective time delays. D is the damping factor and ω_0 is the resonance frequency.

$$G_{ifw} = G_{DRTS} \times G_{D/A} \times G_{amp} \quad (1)$$

$$G_{DRTS} = e^{-(T_{DRTS})s} \quad (2)$$

$$G_{D/A} = e^{-(T_{D/A})s} \quad (3)$$

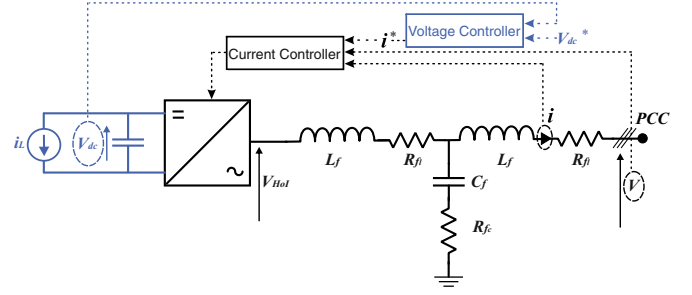


Fig. 2. Schematic of Inverter

$$G_{amp} = \frac{e^{-(T_{amp})s}}{(1/\omega_0)s^2 + (2D/\omega_0)s + 1} \quad (4)$$

In the feedback path G_{ifb} , the transfer functions of the sensor, A/D converter, and the low-pass filter are considered as follows, where T_{sensor} and $T_{A/D}$ are the time delays of the sensor and A/D converter and ω_c is the cut-off frequency of the low-pass filter:

$$G_{sensor} = e^{-(T_{sensor})s} \quad (5)$$

$$G_{A/D} = e^{-(T_{A/D})s} \quad (6)$$

$$G_{filter} = \frac{\omega_c}{s + \omega_c} \quad (7)$$

$$G_{ifb} = G_{sensor} \times G_{A/D} \times G_{filter} \quad (8)$$

Using the equations for the forward and feedback path, the current at PCC can be described depending on the coefficients H_{grid} and $Y_{grid} = 1/Z_{grid}$, shown in equation (9).

$$i = \underbrace{-\frac{1}{G_{ifb} \times Z_s}}_{H_{grid}} V_s + \underbrace{\frac{1}{G_{ifb} \times Z_s \times G_{ifw}}}_{Y_{grid}} V \quad (9)$$

The inverter impedance describes the relationship between the voltages and currents of the inverter and the PCC. It includes the transfer functions of the LCL filter, the cascaded controller, the grid-following converter, and the DC link. The cascaded controller consists of an inner current controller and an outer voltage controller. The structure of the inverter can be seen in Fig. 2, where the blue-marked components show the newly added components in this paper.

According to Fig. 2, the current i at PCC can be described as a superposition of the LCL transfer functions seen from the grid side $Y_{LCL,V}$ and the inverter side $Y_{LCL,HoI}$.

$$i = Y_{LCL,HoI} V_{HoI} - Y_{LCL,V} V \quad (10)$$

Fig. 3 shows the structure of the cascaded controller of the inverter. According to this figure, the voltage at the HoI depends on the DC link voltage V_{dc} , the reference of the DC link voltage V_{dc}^* , and the voltage and current at PCC:

$$V_{HoI} = [((v_{dc}^* - v_{dc} T_d) G_{PI,V} - i T_d) G_{PI,I} + V T_d] T_d \quad (11)$$

The DC link voltage can be expressed by the power equation of the power injected from the grid side in the DC link over

TABLE I
PHIL SIMULATION PARAMETER

T_{DRTS} [μs]	T_{Amp} [μs]	$T_{A/D}, T_{D/A}$ [μs]	T_{Sensor} [μs]	T_d [μs]	$\omega_0/(2\pi)$ [MHz]	$\omega_c/(2\pi)$ [kHz]	L_s [mH]					
50	1.5	3	3	50	1.131	12.57	3.4					
L_f [mH]	C_f [μF]	R_s [Ω]	R_{fl} [Ω]	R_{fc} [Ω]	D	v_{dc0} [V]	v_{ig} [V]	$k_{p,i}$	$k_{i,i}$	$k_{p,v}$	$k_{i,v}$	C_{dc} [μF]
2.4	12	0.143	0.1	1.5	0.9	800	310	3	50	0.1	1	200

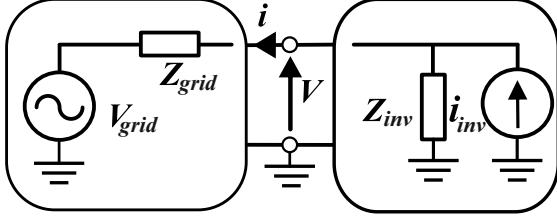


Fig. 4. Impedance Model of P-HIL Setup [17]

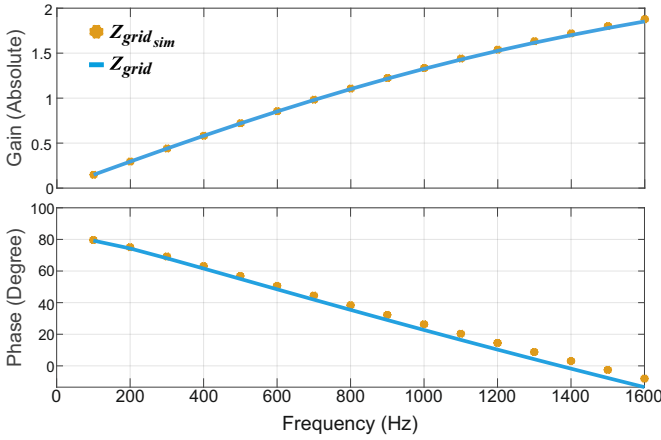


Fig. 5. Grid Impedance Verification

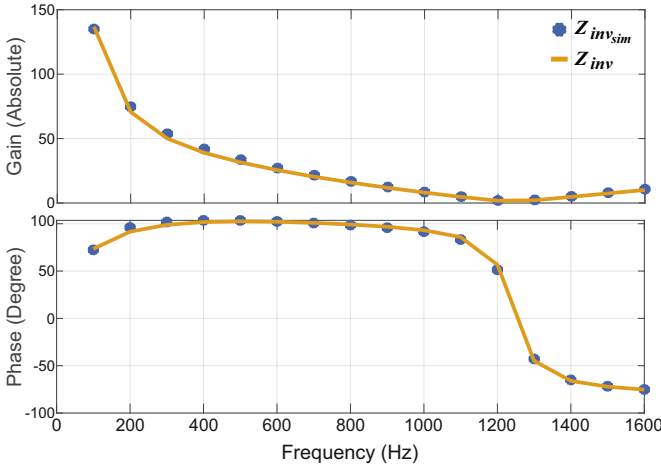


Fig. 6. Inverter Impedance Verification

used for stability assessment, which examines if the point $[-1, j0]$ in the Nyquist plot is encircled or not. For $k = 0.5$, the graph in the Nyquist plot encircles the point $[-1, j0]$, which

indicates that the system is unstable. As the current measured at PCC in the benchmark is unstable, the indicated instability of the P-HIL setup by the Nyquist criterion is confirmed. When changing k to 0.7, the Nyquist graph does not encircle the point $[-1, j0]$, and the setup is, therefore, stable, confirmed by a stable PCC current waveform measured in the benchmark.

As this paper focuses on the impact of the DC port on the stability of the P-HIL setup and considers the DC port dynamics, it is necessary to change the DC side parameters as well while assessing the stability. When changing the DC capacitor from 200 μF to 6 μF , the Nyquist criterion indicates stability, as the point $[-1, j0]$ is not encircled in Fig. 7. In contrast to the Nyquist plot, the setup is unstable, as the PCC current waveform shows in Fig. 8. In [15], the stability criterion using the impedance ratio was introduced under the condition that the internal sources are stable. As derived in section II, the internal sources in this setup are V_{grid} and i_{inv} . The dynamics of the DC port are taken into account in this paper, which shows itself in the fact that the DC side components can influence the stability of the modeled sources. Therefore, the internal sources must be checked for stability before the impedance ratio can be used to analyze the stability of the complete setup. The voltage source V_{grid} is stable as it has no right half-plane poles. To check the stability of the current source, the open loop transfer function of the current source is used, which is defined as follows:

$$G_{op} = G_{PI,I} T_d^2 Y_{LCL, HoI} - v_{ig} \frac{3}{2} \frac{1}{v_{dc0}} T_d^5 Z_{cc} G_{PI,V} G_{PI,I} Y_{LCL, HoI} \quad (19)$$

When checking the stability of the current source i_{inv} , it can be seen that it is unstable as the point $[-1, j0]$ in Fig. 9 is encircled. Due to the instability of the current source, the stability of the setup cannot be determined using the impedance ratio.

V. CONCLUSION

Before using a P-HIL setup to test new hardware, stability assessments must be done to avoid damaging the setup. This paper uses the impedance-based stability criterion to present the impact of the source on the stability analysis of a P-HIL setup with a DC/AC converter. The grid and inverter impedances are modeled based on the P-HIL setup to be investigated. Using the modeled impedances, the impedance-based stability analysis is done while changing different parameters of the setup's AC and DC sides. The stability analysis results show that when assessing a DC/AC converter with

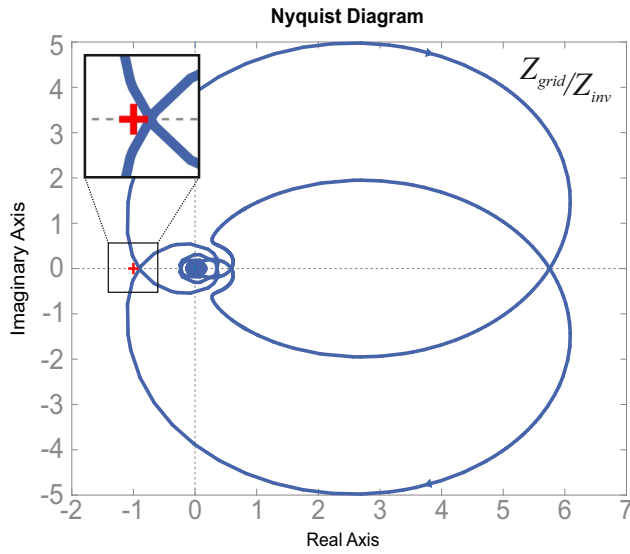


Fig. 7. Nyquist Diagram of Z_{grid}/Z_{inv}

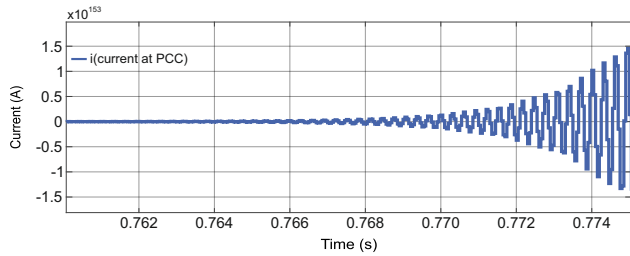


Fig. 8. Time-domain response of inverter current

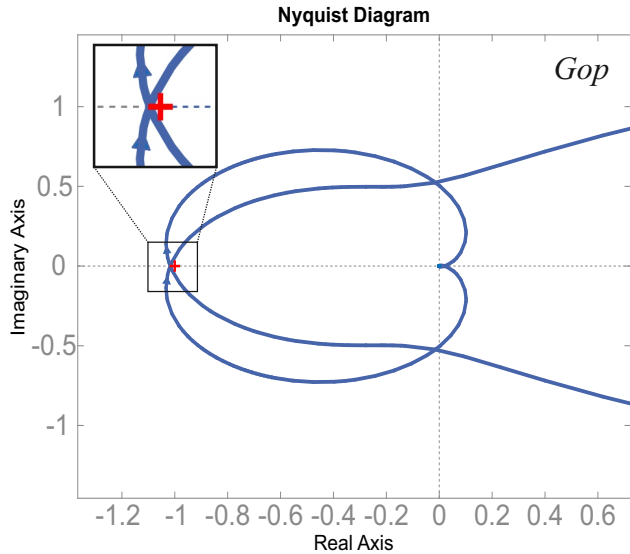


Fig. 9. Nyquist Diagram of G_{op}

a dynamic DC port, it is not sufficient to include only the AC side parameters in the stability analysis. As the DC port components influence the setup's stability, they must also be considered in the stability assessment. Therefore, first, the

internal sources must be checked for stability. If the modeled sources are stable, the impedance ratio can be used to evaluate the stability of the P-HIL setup with a DC/AC converter. The modeled impedances and stability analysis are validated by comparing them with the benchmark of the P-HIL setup in MATLAB/Simulink.

REFERENCES

- [1] D. B. Rathnayake et al., "Grid Forming Inverter Modeling, Control, and Applications," in IEEE Access, vol. 9, pp. 114781-114807, 2021
- [2] L. Ferreira Costa, G. De Carne, G. Buticchi and M. Liserre, "The Smart Transformer: A solid-state transformer tailored to provide ancillary services to the distribution grid," in IEEE Power Electronics Magazine, vol. 4, no. 2, pp. 56-67, June 2017
- [3] J. Carrasco, L. Franquelo, J. Bialasiewicz, E. Galvan, R. PortilloGuisado, M. Prats, J. Leon, and N. Moreno-Alfonso, "Power-electronic systems for the grid integration of renewable energy sources: A survey," IEEE Transactions on Industrial Electronics, vol. 53, no. 4, pp. 1002-1016, 2006
- [4] Chris S. Edrington et al. "Role of Power Hardware in the Loop in Modeling and Simulation for Experimentation in Power and Energy Systems," in Proceedings of the IEEE 103.12, 2015, pp. 2401-2409
- [5] F. Wald, Q. Tao and G. De Carne, "Virtual Synchronous Machine Control for Asynchronous Grid Connections," in IEEE Transactions on Power Delivery, vol. 39, no. 1, pp. 397-406, Feb. 2024
- [6] L. Wang et al., "A Reconfigurable Megawatt-Scale Power Hardware-in-the-Loop Simulation System for Virtual Motors," 2021 IEEE Electric Ship Technologies Symposium (ESTS), Arlington, VA, USA, 2021, pp. 1-5
- [7] F. Reißner and G. De Carne, "Virtual Synchronous Machine integration on a Commercial Flywheel for Frequency Grid Support," in IEEE Transactions on Power Electronics, vol. 39, no. 10, pp. 12086-12090, Oct. 2024
- [8] P. Teske, M. Eggers, H. Yang and S. Dieckerhoff, "Power Hardware-in-the-Loop Testbench for Grid-Following and Grid-Forming Inverter Prototyping," 2022 IEEE 13th International Symposium on Power Electronics for Distributed Generation Systems (PEDG), Kiel, Germany, 2022, pp. 1-6
- [9] G. De Carne, G. Buticchi and M. Liserre, "Current-type Power Hardware in the Loop (PHIL) evaluation for smart transformer application," 2018 IEEE International Conference on Industrial Electronics for Sustainable Energy Systems (IESES), Hamilton, New Zealand, 2018, pp. 529-533
- [10] J. Ihrens, S. Möws, L. Wilkening, T. A. Kern, and C. Becker, "The impact of time delays for power hardware-in-the-loop investigations," Energies, vol. 14, no. 11, 2021
- [11] W. Ren, M. Steurer, and T. L. Baldwin, "Improve the stability and the accuracy of power hardware-in-the-loop simulation by selecting appropriate interface algorithms," in 2007 IEEE/IAS Industrial & Commercial Power Systems Technical Conference, 2007, pp. 1-7.
- [12] M. Bokal, I. Papič and B. Blažič, "Stabilization of Hardware-in-the-Loop Ideal Transformer Model Interfacing Algorithm by Using Spectrum Assignment," in IEEE Transactions on Power Delivery, vol. 34, no. 5, pp. 1865-1873, Oct. 2019
- [13] G. Lauss, F. Lehfuß, A. Viehweider and T. Strasser, "Power hardware in the loop simulation with feedback current filtering for electric systems," IECON 2011 - 37th Annual Conference of the IEEE Industrial Electronics Society, Melbourne, VIC, Australia, 2011, pp. 3725-3730
- [14] F. Ashrafiidehkordi, D. Kottonau and G. De Carne, "Multi-Rate Discrete Domain Modeling of Power Hardware-in-The-Loop Setups," in IEEE Open Journal of Power Electronics, vol. 4, pp. 539-548, 2023
- [15] J. Sun, "Impedance-based stability criterion for grid-connected inverters," IEEE Transactions on Power Electronics, vol. 26, no. 11, pp. 3075-3078, 2011
- [16] L. Xiong, X. Liu, Y. Liu, and F. Zhuo, "Modeling and stability issues of voltage-source converter- dominated power systems: A review," CSEE Journal of Power and Energy Systems, vol. 8, no. 6, pp. 1530-1549, 2022
- [17] F. Ashrafiidehkordi, X. Liu, and G. De Carne, "Impedance-based stability analysis of a power hardware-in-the-loop for grid-following inverter testing," in 2023 IEEE Energy Conversion Congress and Exposition (ECCE), 2023, pp. 1116-1121